

Biophysical Journal, Volume 99

Supporting Material

Single molecule diffusion of membrane-bound proteins: Window into lipid contacts and bilayer dynamics

Jefferson D. Knight, Michael G. Lerner, Joan G. Marcano-Velázquez, Richard W. Pastor, and Joseph J. Falke

Table S1: Mobile fraction (pre-bleaching) of lipid and multi-PH domains

Species	Spots analyzed	Mobile spots	Mobile fraction	Immobile fraction
Lipid (LRB-DOPE)	261	222	~90%	~10%
1PH	105	81	~80%	~20%
2PH	356	209	~60%	~40%
3PH	527	87	~20%	~80%

To estimate the mobile fraction of each species, several areas of membrane were imaged prior to photobleaching, and the number of spots exhibiting significant mobility within 1 second of the first frame of each movie was counted and compared to the number of total spots. Potential sources of immobile particles are discussed in the text.

Table S2: Summary of diffusion constants measured by fitting data from individual movies to cumulative distribution functions

Species	D ($\mu\text{m}^2/\text{s}$)	n (movies)*	n (samples)	n (trajectories)
Lipid (LRB-DOPE)	2.9 ± 0.2	26	8	5115
1PH	2.8 ± 0.2	16	4	1485
2PH	1.5 ± 0.1	16	4	2254
3PH	1.2 ± 0.2	20	8	980
2PH-XL	1.5 ± 0.1	12	3	2052
2PH Δ PIP3	2.7 ± 0.2	16	4	1978

Movies were acquired at either 20 frames/s (50 ms/frame) or 50 frames/s (20 ms/frame). Diffusion was analyzed based on the method of Schütz et al (25) as we described previously (20) (see Methods and legend to Fig. S3). Diffusion constants shown are averages among all movies, with uncertainties ± 1 SD. Measurements were performed on PC/PIP₃ (98:2) membranes at room temperature ($20 \pm 1^\circ\text{C}$) in a near-physiological buffer (see Methods).

FIGURE S1

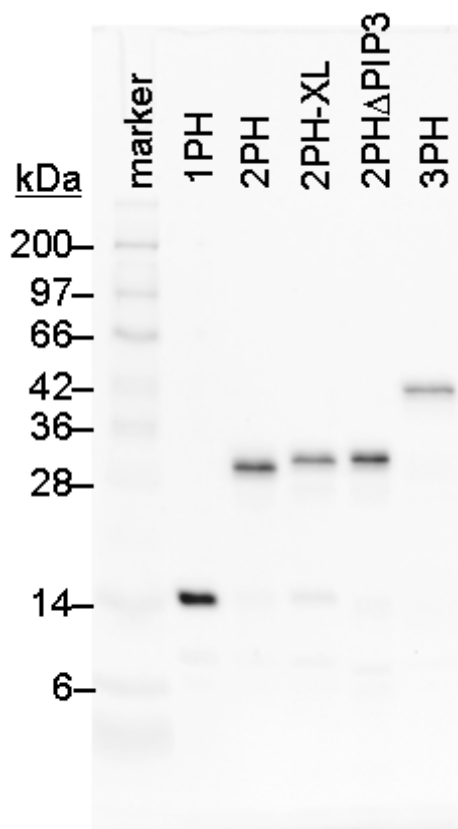


FIGURE S1: Size and purity of proteins used. SDS-PAGE of purified proteins was performed with fluorescence detection. Purity was determined by densitometry analysis using ImageJ. All proteins were found to be $\geq 90\%$ pure except 2PH-XL (80%). Fluorescent MW markers (DyLight 549/649, Thermo Scientific) confirmed that the isolated proteins exhibited the expected sizes. (We note that the preparation of 2PH-XL contained a small level of contamination with a fluorescent molecule the size of 1PH, presumably due to proteolysis of the longer linker, which could potentially lead to overestimation of the diffusion constant. However, this 1PH contaminant would yield a low level of membrane-bound protein since its concentration is low relative to 2PH-XL, and since the dimeric construct binds the membrane ~ 10 -fold more tightly than the monomeric domain as judged by the protein concentration needed to generate a given density of membrane-bound fluorescent particles.)

FIGURE S2

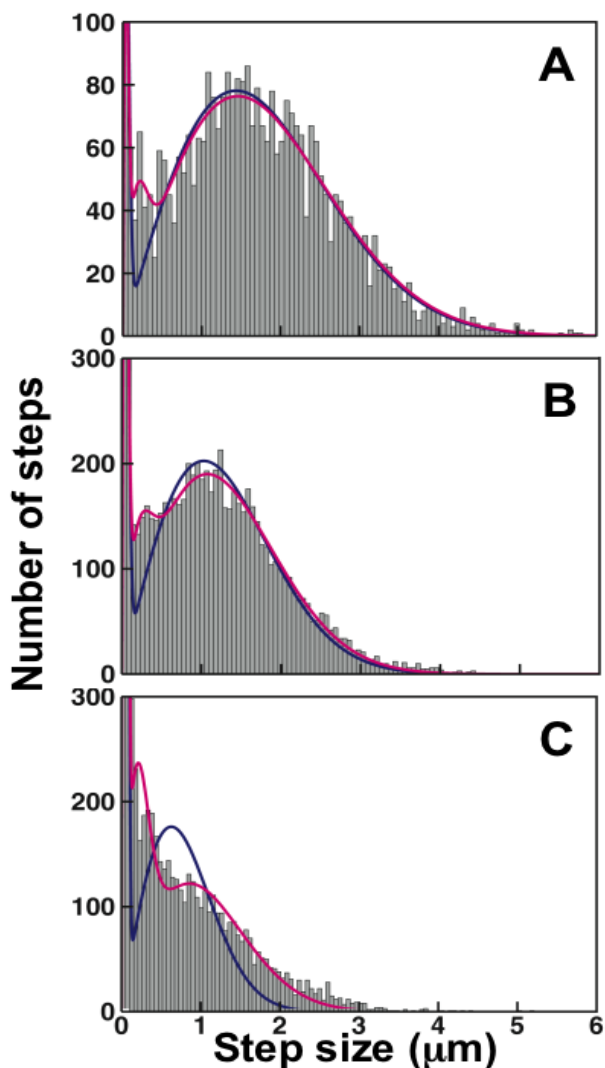


FIGURE S2: Multicomponent analysis of pooled data for 1PH, 2PH, and 3PH. All trajectory data from 50-ms exposure movies of each construct were pooled as described in Methods. Using $\Delta t = 0.4$ s (8 frames), step sizes for (A) 1PH, (B) 2PH, and (C) 3PH were binned into 100 equally-spaced bins to create probability distribution histograms (gray bars). The probability distributions were fit to the sum of 2 Rayleigh distributions for immobile and mobile components (blue line, Eq. 2), or to the sum of 3 Rayleigh distributions for immobile, slow and mobile components (red line, Eq. 3). The 3-component model fits all three data sets well and suggests the existence of a slow component for the 2PH and 3PH constructs as summarized in Table 1. However, it is possible that the slow component arises from particles that interconvert between immobile and mobile states during a trajectory, since simulated data for a particle that interconverts between immobile and fully mobile states on a timescale similar to Δt was found to introduce an apparent slow component and required a 3-component fit. In fact, we do observe particles that stop and restart motion, and this behavior appears to occur more frequently with increasing number of PIP₃-bound PH domains (Movies S1-S3).

FIGURE S3

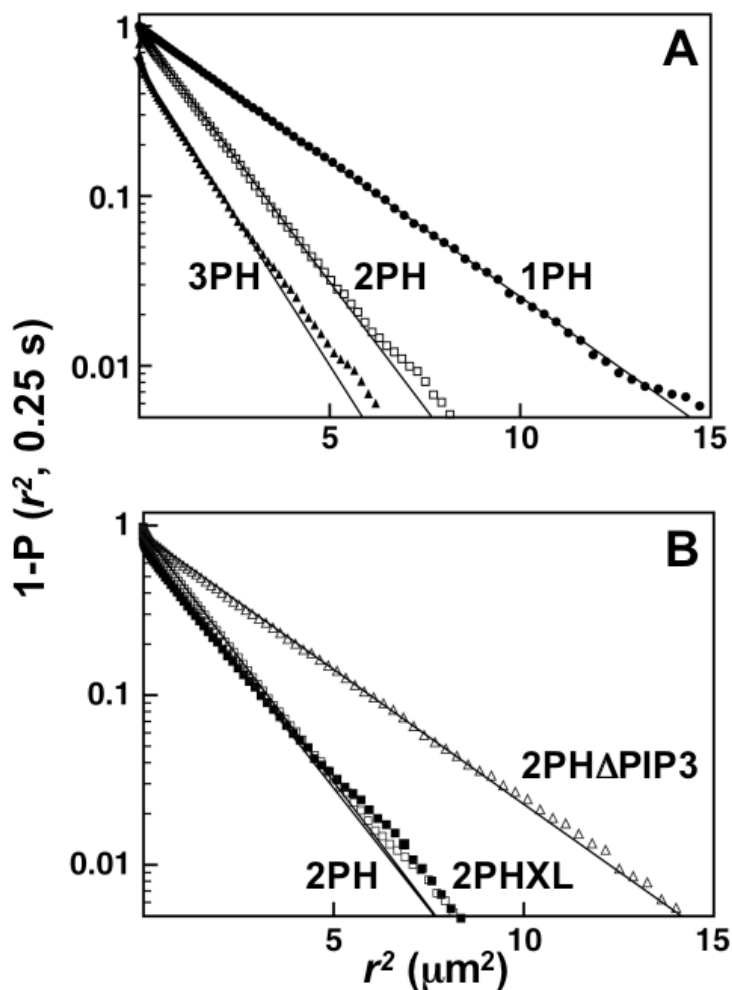


FIGURE S3: Fitting of diffusion data to cumulative distribution functions. For each movie, trajectories with overall $D < 0.1 \mu\text{m}^2/\text{s}$ were removed from analysis and the cumulative probability distributions shown were generated from the remaining trajectories. Cumulative probability distributions represent the probability that a particle moves a squared distance of at least r^2 over the given time interval (here, 0.25 s). In order to further exclude immobile and slow states of trajectories that interconvert between states, distributions were fit (solid lines) to a single exponential decay for all steps $> 0.04 \mu\text{m}^2$. Values of mean square displacement ($\langle r^2 \rangle$) were extracted from fits as described; these are plotted in Fig. 3A-B of the main text (20, 25). Data are shown here for (A) 1PH, 2PH, and 3PH; and (B) 2PH, 2PHXL, and 2PH Δ PIP3. The vast majority of steps fall in an exponential region representing a single, homogeneously diffusing population. Deviations towards higher probability at the greatest r^2 values likely include small populations of states that exhibit incomplete PIP₃ coordination.

LEGENDS FOR SUPPLEMENTARY MOVIES:

Movie S1: Diffusion of 1PH on a PC/PIP₃ (98:2) membrane. Movie is shown in real time (20 frames/s, 50 ms exposure), and contains a representative sequence of 200 frames from a 2000-frame acquisition.

Movie S2: Diffusion of 2PH on a PC/PIP₃ (98:2) membrane. Movie is shown in real time (20 frames/s, 50 ms exposure), and contains a representative sequence of 200 frames from a 2000-frame acquisition.

Movie S3: Diffusion of 3PH on a PC/PIP₃ (98:2) membrane. Movie is shown in real time (20 frames/s, 50 ms exposure), and contains a representative sequence of 200 frames from a 2000-frame acquisition.